

# sNVMe-oF: Secure and Efficient Disaggregated Storage

Marcin Chrapek  
marcin.chrapek@inf.ethz.ch  
ETH Zurich  
Zurich, Switzerland

Meni Orenbach  
NVIDIA  
Santa Clara, USA

Ahmad Atamli  
NVIDIA  
Santa Clara, USA  
University of Southampton  
Southampton, UK

Marcin Copik  
ETH Zurich  
Zurich, Switzerland

Fritz Alder  
NVIDIA  
Santa Clara, USA

Torsten Hoefer  
ETH Zurich  
Zurich, Switzerland

## Abstract

Disaggregated storage with NVMe-over-Fabrics (NVMe-oF) has emerged as the standard solution in modern data centers, achieving superior performance, resource utilization, and power efficiency. Simultaneously, confidential computing (CC) is becoming the de facto security paradigm, enforcing stronger isolation and protection for sensitive workloads. However, securing state-of-the-art storage with traditional CC methods struggles to scale and compromises performance or security. To address these issues, we introduce sNVMe-oF, a storage management system extending the NVMe-oF protocol and adhering to the CC threat model by providing confidentiality, integrity, and freshness guarantees. sNVMe-oF offers an appropriate control path and novel concepts such as counter-leasing. sNVMe-oF also optimizes data path performance by leveraging NVMe metadata, introducing a new disaggregated Hazel Merkle Tree (HMT), and avoiding redundant IPsec protections. We achieve this without modifying the NVMe-oF protocol. To prevent excessive resource usage while delivering line rate, sNVMe-oF also uses accelerators of CC-capable smart NICs. We prototype sNVMe-oF on an NVIDIA BlueField-3 and demonstrate how it can achieve as little as 2% performance degradation for synthetic patterns and AI training.

## 1 Introduction

Storage is the backbone of modern data centers, affecting the performance of applications [55], microservices [56], serverless platforms [57], and the broader X-as-a-Service (XaaS) ecosystem [31]. The cost-effectiveness of storage has been improved by disaggregation [47], which decouples storage from compute, enabling independent scaling and more efficient resource utilization. Disaggregated storage achieves microsecond-level latencies and millions of IOPS through advances such as NVMe over Fabrics (NVMe-oF) [4] leveraging remote direct memory access (RDMA) [42], smart NIC (sNIC) offloading [45, 61], and 200 - 400 Gbit networks.

Simultaneously, security became one of the most critical business determinants for cloud service providers (CSPs) [37, 69, 83]. Confidential Computing (CC) [64, 73] emerged as a de facto standard for the future of data centers. In

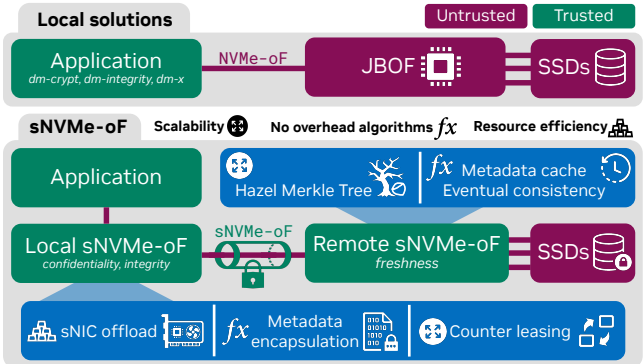


**Figure 1.** An overview of the locally deployed methods and sNVMe-oF with its novel contributions in scalability, algorithms  $\mathcal{fx}$ , and resource efficiency.

CC, tenants can attest that their programs run in secure, isolated runtimes called trusted execution environments (TEEs) [27, 29, 53, 70, 76]. TEEs shield from other tenants and the hypervisor, lowering the threat of data leakage and protecting even from hardware administrators. These are essential for data-sensitive industries, such as healthcare, finance, and artificial intelligence, which are increasingly interested in leveraging cost and scalability benefits of CSPs.

Secure storage is essential for the guarantees of any CC system [10]. However, CC changes the typical threat model for storage. Existing cloud storage solutions offered by cloud service providers (CSPs) only offer confidentiality through basic disk encryption with constant initialization vectors (IVs). Such protection is insufficient for CC, which requires unique IVs and two additional properties [30]: integrity (data is unmodified), freshness (data is not outdated). Tenant-deployed solutions designed for local deployments, such as *dm-x* [25], relying on *dm-crypt* and *dm-integrity*, offer some of these guarantees. However, non-trivial challenges arise on the control and data paths when naively introducing modern high-performance disaggregation to these solutions.

We discuss these issues in depth in Section 3 and identify key limitations, including low scalability, performance degradation, and high CPU utilization. These impact security,

require unrealistic synchronizations that would congest the network, and can reduce overall throughput by up to 50% while driving CPU usage above 80%. To address these issues, we propose sNVMe-oF, a first-of-its-kind secure disaggregated storage system that extends the existing NVMe-oF capabilities to satisfy the CC threat model in a scalable, performant, and secure manner.

We achieve this by introducing three key innovations summarized below and in Figure 1. First, we introduce a scalable control path. Scalability is critical, as modern storage solutions consistently grow in size as SSD density doubles every 1.5 years [1]. Solutions combining multiple SSD drives already reach 1 PB, and some vendors discuss developing single 1 PB drives [7]. A key observation enabling our control path is that disaggregating the storage also opens up a new opportunity to disaggregate the Merkel Tree (MT), which is commonly used to provide freshness. As this necessitates increasing the threat boundary, we introduce a novel control flow that distributes the necessary protections. We perform MT management and verification on the storage node, saving communication overhead on the data path and addressing scalability issues related to freshness. sNVMe-oF also provides an IV leasing strategy enabling strict confidentiality on PB-sized storage.

Second, we optimize the data path, building on a key observation that many algorithmic overheads in existing solutions can be eliminated. Instead of modifying the NVMe-oF protocol, which might require hardware changes, sNVMe-oF relies on encapsulation to enable security and can be deployed on existing systems. For that, we leverage a new design trend in data center NVMe: large block metadata as part of the logical block address (LBA). sNVMe-oF uses metadata to achieve crash-protected integrity and confidentiality at a negligible cost, and to replace transport layer solutions such as IPSec [35], minimizing repeated encryptions on the critical path. sNVMe-oF also introduces a novel tree organization for freshness, which we have named Hazel MT (HMT). HMT addresses the shortcomings of a typical MT when applied to PB-scale drives by modifying its storage, verification, and update methods. HMT enables asynchronous writes and read path verification at a negligible cost. HMT also supports freshness crash-protection through a proposed hardware extension. All these cost a storage overhead of just 1.76%.

Third, we improve resource efficiency by leveraging the key observation that infrastructure tasks can be offloaded to network-specific accelerators such as smart NICs (sNICs), thereby alleviating CPU pressure [6, 78]. As this requires extending the trust boundary onto the sNIC, we exploit a new trend that equips them with CC capabilities [50]. We use CC-capable sNICs as infrastructure security managers and as accelerators designed for network line rates. While we deploy sNVMe-oF on an sNIC to alleviate resource pressure and enable features such as GPU direct, sNVMe-oF can be

deployed as a CPU service. It can also be deployed in a non-disaggregated setup, as our innovations are still applicable.

We prototype and evaluate the performance of sNVMe-oF on an NVIDIA Bluefield-3 leveraging Storage Performance Development Kit (SPDK) [87] and NVIDIA DOCA [65]. We display that integrity can cost as little as 2% performance once saturation is achieved. We also show how our optimizations allow freshness to achieve similar overheads.

### In summary, our contributions are:

1. Designing sNVMe-oF, a novel secure disaggregated storage system providing confidentiality, integrity, and freshness under the CC threat model. We introduce novel ideas on the control path, such as disaggregated MT and IV leasing.
2. Introducing algorithmic enhancements of data path performance through encapsulation, leveraging NVMe metadata to create novel zero-overhead paths and avoid redundancy with IPSec. We also present HMT, a new MT type offering optimized reads and writes.
3. Prototyping and open-sourcing sNVMe-oF on top of Nvidia Bluefield 3, offloading integrity checks to the sNIC, demonstrating how to combine SPDK and DOCA, and proposing a minimal hardware extension for freshness and crash protection.
4. Evaluating sNVMe-oF on a real system, showing as little as 2% overhead on synthetic benchmarks and a machine learning training pipeline.

## 2 Background

**Storage disaggregation:** Tenants are typically provided access to a local, small SSD and a remote just-a-bunch-of-flash (JBOD) array. JBODs frequently comprise a processor (CPU or sNIC) [8, 85], domain-specific accelerators (e.g., RAID), and up to 36 NVMe SSDs. NVMe SSDs comprise sectors that are the smallest read and write units, and can have associated metadata. Typically, sectors are either 512 B or 4096 B, with metadata of 0-8 B for customer SSDs and up to 64 B for data center ones. NVMe SSDs are disaggregated via NVMe-oF, an extension of the NVMe protocol that enables high-speed, low-latency data transfer between hosts and storage devices across the network [4]. Recently, NVMe-oF incorporated several security mechanisms, such as protecting transport with TLS or IPSec encapsulation. However, securing the transport is not a silver bullet, as in CC, the data stored at rest must also be protected.

**Secure cloud storage:** CSPs offer secure storage solutions in the form of full disk encryption [9, 20, 63]. These solutions are typically based on AES-XTS [33] with the encryption tweak based on the sector number. Such implementation opens up chosen-ciphertext attacks [52, 68], as encrypting the same data at the same sector with an unchanged tweak will produce identical ciphertexts. Furthermore, these solutions do not verify data integrity and are not attestable. They

also do not provide the freshness of data, which guarantees protection against replay attacks in which an adversary replaces the current value with a stale one. Such a temporal difference indirectly breaks integrity but is not detected by simple hashing. Offering only confidentiality is insufficient in CC for which trust, integrity, and freshness are security critical [60], especially in long-term storage. Tenant local solutions like *dm-x* [25] only partially address these issues.

**Local secure storage solutions:** *dm-x* introduces confidentiality, integrity, and freshness. Confidentiality is enabled by encrypting sectors with Linux’s *dm-crypt*. Integrity is provided through *dm-integrity* with cryptographic hashes. *dm-crypt* and *dm-integrity* are recommended for TEEs [10]. On top of these two solutions, *dm-x* [25] provides freshness by employing an MT. MTs are based on hashes computed for integrity protection. Hashes of data constitute MT leaves. The branching factor of an MT defines how many children are hashed together to obtain parents. Changes in the data cause a hash recalculation on each level, which ultimately updates the root. This guarantees online freshness, as changes to old values will manifest themselves with a different node value somewhere in the tree during subsequent read verification. The root must be placed in persistent and secure storage to enable offline freshness. The main issue with these solutions is that they were designed to secure *local storage rather than remote one*, and operate from the kernel, disabling features such as GPUDirect storage [3].

### 3 Inadequacy of local secure storage

While providing confidentiality, integrity, and freshness, *dm-x* and its dependencies (*dm-crypt*, *dm-integrity*) struggle when naively applied to protect disaggregated storage for three reasons: confidentiality and integrity scalability, resource and algorithmic overheads, and freshness scalability.

#### 3.1 Confidentiality and integrity at scale

The first step toward deploying a fully CC-compliant storage cloud solution is eliminating equality attacks in existing confidentiality mechanisms and enabling integrity. The former can be addressed by ensuring the encryption tweaks or initialization vectors (IV) do not repeat, while the latter can be achieved by introducing cryptographic hashes.

Encryption schemes like AES [32, 33, 66] provide confidentiality by dividing data into blocks and processing them with a secret key and a unique IV. Reusing IVs with the same key introduces collisions that weaken security. For some ciphers, such as AES-XTS, this only leaks equality information. However, for many authenticated encryption with associated data (AEAD) algorithms, such collisions represent severe security vulnerabilities. For instance, collisions in AES-GCM are catastrophic, leaking plaintext data [43]. As we show in Section 3.2, AEAD algorithms achieve integrity considerably more efficiently than combining IV-resilient ciphers with

Algorithm	Block size [bits]	IV size [bits]	Write capacity	
			Random	Sequential
AES-XTS	128	128	4.2 PB	$5.4 \cdot 10^{24}$ PB
AES-GCM	128	96	64.1 GB	$1.3 \cdot 10^{15}$ PB
AEGIS128L	256	128	8.4 PB	$1.1 \cdot 10^{25}$ PB
ChaCha20	512	96	256.2 GB	$5.1 \cdot 10^{15}$ PB

**Table 1.** Different encryption algorithms with the total amount of data that can be safely written using a single key. We use NIST guidelines for collision probabilities  $p(n, d)$  and  $n \approx \sqrt{-2 \cdot 2^d \log(1 - p(n, d))}$ , with constant cipher parameters:  $n$ , number of encryptions,  $d$ , number of IV bits.

separate hashing, making unique IVs essential. National Institute of Standards and Technology (NIST) specifies the maximum safe probability of collisions as  $2^{-32}$  [43].

A common approach to implementing confidentiality is allocating each storage partition a key and using the sector number as the IV. Such an approach introduces collisions when writing to the same sector, since the key remains constant. Using the sector number as an IV was attractive because it eliminated the need to store additional information per sector. However, when introducing integrity hashes, side storage becomes unavoidable, adding algorithmic overhead (Section 3.2). Two alternatives provide unique IVs on every write: random generation and counters. Once unique values are exhausted, a new encryption key must be provisioned.

**Random IV:** Randomly sampled IVs are constrained by the birthday paradox, which limits the number of writes per key before collisions become likely. Table 1 shows maximum safe write volumes for a single key. In the best case, random IVs permit up to 8.4PB of data using the same key. While this suffices for a local SSD, disaggregated PB-scale storage requires considerably more. As an SSD’s average lifetime is 10,000 write cycles, the necessary write capacity is in thousands of PBs. This limitation necessitates frequent key rotation. Existing approaches do not address questions such as how to synchronize write counts of a given key across multiple tenant instances, how to record which blocks were written with which keys, how to generate the keys and synchronize them between tenant instances, and where to persistently store them in a CC compliant manner.

**Counter IV:** Increasing a counter during each write provides IVs not bound by the birthday paradox. While almost limitless, counter IVs as provided by *dm-crypt* are not scalable. Multiple tenant instances must coordinate to avoid overlapping counters, requiring synchronization across instances. Such coordination is manageable at a small scale but quickly becomes infeasible in a datacenter setting, where all-to-all synchronization would severely slow the data path and require tenant instances to trust one another.

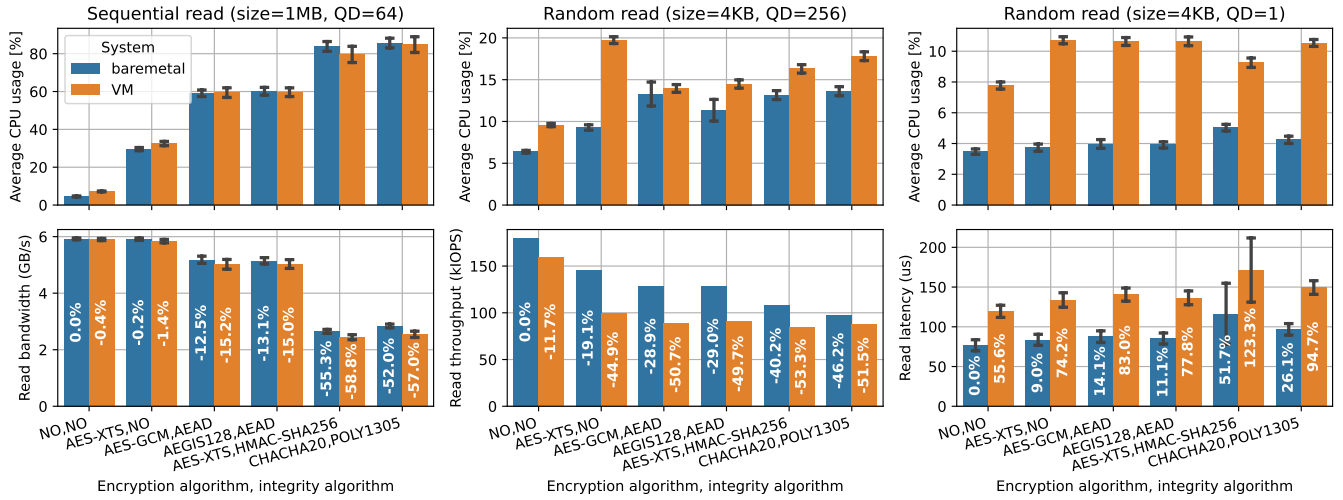


**Figure 2.** Read throughput, IOPS, and latency across different encryption and integrity algorithms with average CPU usage on a hyperthreaded system (50% CPU usage involves all physical cores). Overheads are relative to unprotected bare metal.

**sNVMe-oF** Scalability, therefore, demands a separate control path and infrastructure not provided by existing systems. We design a scalable counter-leasing protocol combined with a key management framework for derivation and storage. This enables multiple tenant instances to use disaggregated JBOFs with per-partition counter allocation without incurring synchronization performance overheads.

### 3.2 Resource and algorithmic overheads

Another issue with introducing integrity is that it costs performance and resources. Figure 2 shows throughput, input-output operations (IOPS), and latency for sequential and random reads of varying sizes and queue depths (QD). We display these across different encryption (*dm-crypt*) and integrity (*dm-integrity*) algorithms along with CPU usage. Section 6.1 provides further setup details.

While AES-XTS confidentiality could provide raw disk performance, even in our single SSD setup, it consumes about 30% CPU. Adding integrity protection pushes overheads to 50% for AEAD algorithms and 80% for algorithms computing sequentially integrity and encryption, without accounting for freshness. As the CPU becomes saturated, the performance also suffers, especially in the case of combined algorithms, where the overheads can reach up to 50%. Such a high CPU usage dedicated to security operations is expensive and prevents efficient parallel data processing. These overheads would be exacerbated in JBOFs, which can deliver several times the throughput of our testbed.

Overheads arise not only from excessive resource usage but also from algorithmic bottlenecks. Synchronous CPU accelerators (e.g., AESNI) block parallel request processing,

kernel context switches add latency, and integrity metadata introduces further I/O. Specifically, *dm-crypt* and *dm-integrity* place integrity hashes and non-constant IVs that require additional storage in separate metadata sectors. Thus, reads require an additional read of these sectors, and writes an additional read-modify-write. Such a design reduces IOPS, increases latency, and necessitates journaling to enable crash protection. As journaling requires writing the data also to the journal, write performance can be reduced by up to 50%. *dm-x* similarly uses journaling for freshness crash protection, and updates and verifies the MT on the critical path. While *dm-crypt* in the 6.14 kernel release introduces support for NVMe metadata, this only stores hashes and not the IVs.

**sNVMe-oF** We address these algorithmic bottlenecks by leveraging NVMe metadata to its full potential: storing both IVs and hashes, supporting network protection, and enabling a fast freshness verification path. To eliminate CPU overhead and improve performance, we move integrity operations off the host kernel - where *dm-crypt* and *dm-integrity* reside - and onto modern sNICs, which are on the critical data path in either case. Unlike synchronous x86 CPUs, sNICs provide asynchronous cryptographic accelerators designed for line-rate processing at lower power [39] and enabling secure operations to run in parallel with application requests.

### 3.3 Freshness at scale

The final necessary guarantee is freshness, but ensuring it at scale is challenging. *dm-x*, designed to run on a tenant instance, requires global consistency across all instances sharing a block device. If multiple instances issue writes concurrently, they must coordinate to maintain a coherent MT. For example, if one instance writes sector zero while another writes sector one, both must synchronize to update

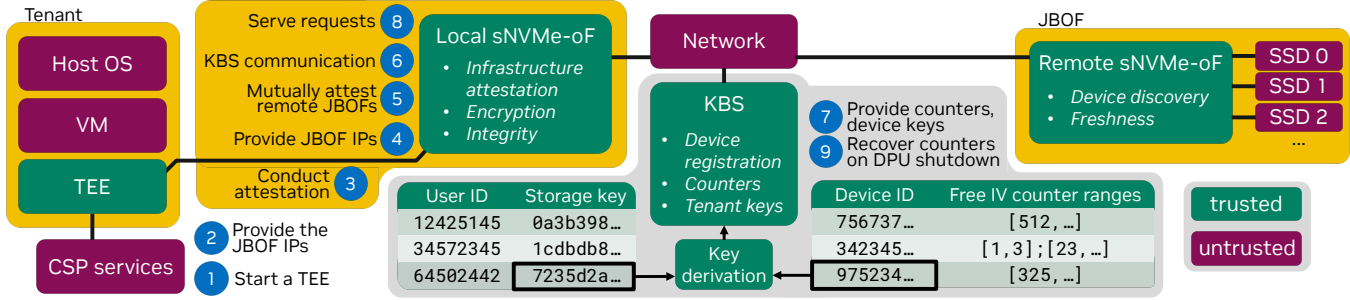


**Figure 3.** An overview of sNVMe-oF’s control flow with multiple stages of attestation, key derivation, and counter leasing.

the parent without conflicts. Such coordination requires secure state sharing, designing a mechanism to persistently store the root of the fresh tree, mutual trust between tenants, and frequent cross-instance communication. All of these issues add network overhead and slow the critical path.

**sNVMe-oF** addresses this by disaggregating the integrity tree to the JBOF and outlining a protocol that ensures trust and supports multiple tenants. We further propose a novel HMT, which modifies typical verification and update algorithms to be multithreaded, cached, and eventually consistent. These create fast read and write paths without synchronization, minimizing the performance overheads.

## 4 Design of sNVMe-oF

Our design focuses on two principles: performance and scalability. These make our solution practical while guaranteeing critical security properties of confidentiality, integrity, and freshness. We present our solution in the most generalizable form possible. This allows us to reach the broadest audience while leaving the flexibility to practitioners. For example, if the network is freshness protected (e.g., Ultra Ethernet encryption [40]), sNVMe-oF’s network freshness header is surplus, allowing for more IV and key ID bits. We first outline our threat model and follow with control and data paths.

### 4.1 Threat model

We adopt a standard CC threat model [64] with both privileged adversaries (e.g., a data center administrator) and unprivileged ones (e.g., like other tenants). Adversaries might be local (on participating nodes) or remote (on the network), and can observe, replay, or tamper with control- and data-plane requests and responses. sNVMe-oF’s primary goal is to protect data at rest on untrusted, disaggregated storage devices serving TEEs, ensuring confidentiality, integrity, and freshness. Following prior work such as dm-x [25], we do not trust the storage devices themselves.

We assume adversaries that may attempt replay or modification attacks, but cannot compromise TEE execution through side channel or transient-execution attacks [34]. While these may expose TEE information, they are orthogonal to our work. We also do not focus on denial of service

attacks, which would violate the service-level agreement and reveal privileged attackers. All sNVMe-oF services are assumed to run inside attested, vulnerability-free TEEs, with access to a small trusted non-volatile memory for storing persistent security-sensitive state (see Section 4.3.1).

### 4.2 Control path

Figure 3 shows the overview of sNVMe-oF’s control path with untrusted (burgundy) and trusted (green) entities. The latter are brought into the trusted computing base (TCB) through attestation. We differentiate two types of sNVMe-oF instances: local and remote. These are used for different purposes, as explained in the Data Path description. We split the control path into three main phases: establishing trust, initializing security, and operation.

**4.2.1 Establishing trust.** sNVMe-oF starts with the CSP scheduling a TEE on the corresponding host ①. Once the TEE starts, it fetches the details of JBOF IPs from a CSP service ②. In the meantime, TEE attests the local sNVMe-oF instance ③. Once the attestation is concluded, the full JBOF IPs are provided ④. The local sNVMe-oF uses these to open connections through mutual attestation [26, 59] ⑤.

A central idea we introduce at this step is that the local instance also functions as a trust gate for the infrastructure. It not only secures its environment but also extends trust to the rest of the storage network, relieving the tenant from this responsibility. The local sNVMe-oF service enforces network security and creates trust with remote sNVMe-oF instances and the Key Broker Service (KBS). For that, these services conduct mutual attestation between each other, as they need to ensure both sides are in the correct state.

Such an approach has performance advantages over the tenant attesting each agent in the network. As the sNVMe-oF service handles these remote attestations, it can conduct them at boot time and keep alive the already opened secure connections (e.g., TLS). The tenant does not need to additionally attest the KBS, and potentially tens to hundreds of devices, each taking at least several milliseconds [62]. The connections to JBOFs can also be opened preemptively if the CSP knows it will allocate specific hosts to certain

JBOFs. This minimizes the initialization cost of sNVMe-oF, which can reach zero in the optimal cached scenario, which is crucial for short-lived workloads affected by startup overheads, such as Function-as-a-Service (FaaS) [28].

The local sNVMe-oF service also provides the tenant identity to the KBS 6, leveraging the connection opened at boot and kept alive. KBS yields security details necessary for starting operation 7. Steps 4 and 5 are independent from 3 and 6, and can be conducted in parallel.

**4.2.2 Initializing security.** The security initialization relies on the KBS providing two pieces of information: per-device counters and tenant storage keys.

**Counter leasing:** sNVMe-oF obtains unique IVs through a counter-leasing protocol. When a remote sNVMe-oF instance discovers a new SSD device, the KBS starts a  $b$  bit range by creating a list per device:  $[(0, 2^b)]$ . Any sNVMe-oF service that would like to access a storage device sends a request to the KBS with the appropriate device ID. The KBS then leases a range of counters corresponding to 1TB; a range large enough to avoid requesting new ones frequently. Using a counter allows sNVMe-oF to allocate an astronomically large number of such ranges (e.g.,  $1.3 \cdot 10^{18}$  for AES-GCM), which can cover SSD lifetime without refreshing keys. The space requirement for such a counter list grows with the number of SSD devices rather than user partitions. Local sNVMe-oF service caches these counters as long as possible, even after the shutdown of the associated TEE. This ensures multiple tenant instances can be spawned on the same host without repeatedly leasing and returning the same counter ranges. If a range needs to be evicted, sNVMe-oF sends it back to the KBS for reuse, even if partially used. The KBS adds it to its per-device list, ensuring compaction. The KBS always returns 1TB of write capacity from the ranges, which might mean many smaller subranges are provided.

**Key management:** sNVMe-oF also manages keys necessary for confidentiality and integrity guarantees 7. Instead of storing user-partition keys, we base our management on key derivation. A user-device key  $k_d$  can be derived from a cryptographic hash function  $H$  for a device with ID  $i$ , and a tenant storage key  $k_s$  leveraging a HMAC [48]  $k_d = \text{HMAC}_{k_s}(i) = H((k_s \oplus opad) || H((k_s \oplus ipad) || i))$  with  $\oplus$  representing the XOR operation,  $||$  concatenation, and  $opad$ ,  $ipad$  outer and inner padding, consisting of repeated  $0x5c$  and  $0x36$  correspondingly. Unique identifiers such as SSD EUI64 can be used as the device ID  $i$ .

We placed key derivation on the KBS, as this limits potential exposure of the master tenant key in case of a data leakage. Such isolation is better than in local solutions such as *dm-crypt*, which would require a global tenant storage key. We also decided to operate on the level of devices rather than NVMe controllers, namespaces, or other partitions, as any change to these (e.g., switching controllers) would require additional tracking and potential full disk re-encryption.

**4.2.3 Operation.** After initializing the secure state, sNVMe-oF moves to data plane operation, serving requests 8. On shutdown, sNVMe-oF service returns the counter ranges to KBS 9, erases local information, and closes connections.

### 4.3 Data path

sNVMe-oF minimizes the overheads on the critical data path. We leverage a key concept of NVMe metadata to store secure information, without modifying the NVMe-oF protocol. Figure 4 shows the encapsulations that sNVMe-oF introduces, including data fields and sector layouts.

Each SSD is split into two distinct sections: metadata and data. Data sectors hold ciphertexts, and their metadata contains hashes, IVs, key identifiers, and freshness caching information used for the fast read path. We group  $S$  data sectors into *data sets*. Each data set has a corresponding metadata sector placed at the beginning of the SSD. Metadata sectors hold aggregated IVs of data sectors and serve as an on-disk cache to optimize freshness.

For an SSD with  $B$  blocks, there are  $D = \lceil B/S + 1 \rceil$ <sup>1</sup> data sets. A data sector  $i$  is placed in the physical sector  $D + i$  and the corresponding metadata at physical sector  $\lfloor i/S \rfloor$ , with an in-sector IV offset of  $i \bmod S$ . We calibrate  $S$  such that as many IVs as possible fit in one metadata sector. For a typical IV of 12B and a sector size of 4096B,  $S = 340$ , yielding sNVMe-oF's overhead on storage of only 0.29% and about 2.94TB of metadata for 1PB of capacity.

**4.3.1 Write path.** Writes start at the TEE as a request consisting of data, device ID, and the sector number. The request is then encapsulated by a security protocol (e.g., PCIe's TEE Device Interface Security Protocol (TDISP) [67]) and is transported to the local sNVMe-oF service, which encrypts and integrity protects it.

**Confidentiality and integrity:** Combining sequentially integrity and encryption algorithms adds considerable overhead (Section 3). Thus, leveraging an AEAD algorithm  $E$ , sNVMe-oF obtains ciphertext  $C$  and integrity hash  $H_i$  as:

$$C, H_i = E(k, \underbrace{\text{sector number}, \text{IV}, \text{write data}}_{AD}, \underbrace{\text{plaintext}}_{\text{AD}}) \quad (1)$$

where  $k$  is a key derived from the KBS provided tenant-device key  $k_d$  as  $k = \text{HMAC}_{k_d}(\text{key ID bits})$ . Including the sector number ensures the sectors cannot be replaced with each other without detection. The device-specific key enforces that the writes to the same sector with the same IV vary for different disks. After each encryption, the IV is increased by the number of encryption blocks (e.g., 256 for 4096B sectors and AES-GCM). While not strictly necessary from a security perspective, including the key ID enables easy key rolling.

**Network freshness:** Disaggregating the freshness protections to the remote side is crucial to enable scalability.

<sup>1</sup>Ignoring the case  $B \bmod S + 1 = 1$  where  $D = \lfloor B/S + 1 \rfloor$

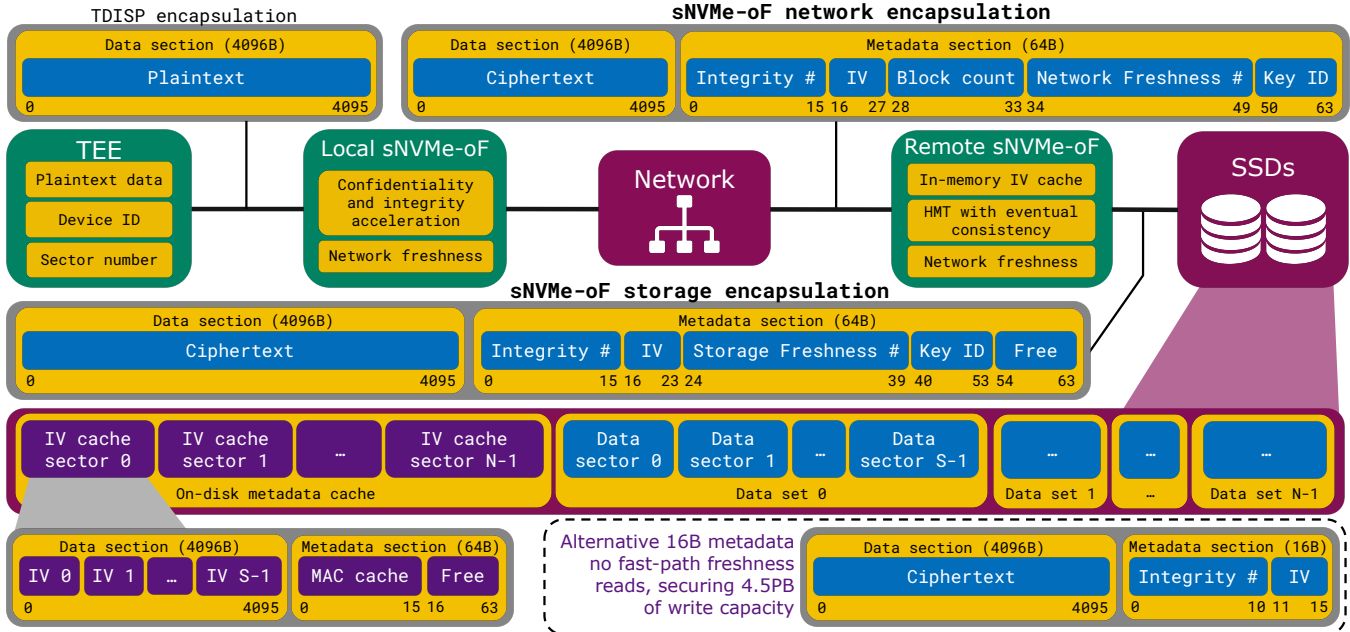


**Figure 4.** The pipeline of requests and how sNVMe-oF creates an encapsulation at each layer to provide security. The SSD zoom-in shows the layout of sectors that sNVMe-oF applies to the underlying SSDs.

However, this necessitates protecting sent sectors as sNVMe-oF operates in a CC environment. While IPSec is the first intuitive way to secure in-network transport, it has considerable drawbacks in our use case. It adds latency to the critical path and decreases the throughput. Furthermore, IPSec has problems with NVMe security as it adds protections on a per IP basis [80], making different services share the same protections. Instead of using IPSec, sNVMe-oF leverages already applied protections. Data confidentiality and integrity are already provided by local sNVMe-oF, and protecting headers adds little value besides out-of-scope DoS attacks. However, freshness needs to be guaranteed over the network, for which sNVMe-oF uses windowing.

Once a secure channel is opened between the local sNVMe-oF and the remote JBOF, the sNVMe-oF instances agree on a communication key  $k$  and a pair of random start counters, one for sending and one for receiving. Writes use the former to obtain a block count  $j$  and compute a network freshness hash  $H_n$  per sector of each request as  $H_n = \text{HMAC}_k(IV||j)$ , with  $||$  representing concatenation.  $H$  is then placed into the corresponding sector's metadata. As  $j$  is 48 bits,  $k$  needs rolling at most every 1.4 years, assuming a continuous 200Gbps usage. Hashing only the IV does not add substantial overhead and is secure, as it is cryptographically bound with the data through  $H_i$ . Through this we avoid repeated encryption and integrity protection at the cost of increased metadata usage. The network freshness is then verified at the JBOF using a sliding window method: writes with a counter

at most  $T$  lower than the current maximum seen are accepted.  $T$  is selected to enable asynchronous packet delivery.

**Storage freshness:** The data must then be committed to the drives and the freshness tree. sNVMe-oF introduces the Hazel Merkle Tree (HMT). Similar to a Bonsai MT [72], HMT uses IVs instead of data for hashing, reducing MT's compute and memory footprint. However, it considerably differs in **storage**, **verification**, and **update** methods. HMT leverages two novel concepts: LBA metadata for fast reads and the introduction of eventual consistency for fast writes.

**Storage:** Apart from its root, an MT in  $dm-x$  is stored entirely on disk. Loading parts of the tree adds a non-deterministic latency, reduces IOPS, and throughput. On the other hand, storing the whole tree in memory is expensive. Given an SSD with  $N$  sectors and  $B$  bytes per hash, such a tree is at least  $B(N + 1)$  bytes (branching factor  $N$  and a single root node). For a 1PB drive  $N = 244 \cdot 10^9$  and a typical hash of  $B = 16B$ , the tree has a size of 3.9TB. It is expensive to equip JBOFs with such a large memory.

To address this HMT is created leveraging two branching factors: one for the leaf data  $D_d$ , and one for the tree  $D_t$ . We store the tree in memory without the underlying zeroth level, which contributes most to its size. This allows HMT to scale considerably better as the in-memory part of the tree is only  $B(N + 1)/D_d$ . As mentioned in Section 4.3, we batch  $S$  IVs in a single metadata sector on the SSD. We set  $D_d = S$ , making the size of the tree manageable. For example, for 1PB, and  $S = 340$ , the tree size becomes at least 11.5GB, which can fit even on a relatively small memory of a sNIC.

This optimization is crucial for performance as it allows us always to maintain the tree without data leaves in memory, enabling the zero-overhead read path (Section 4.3.2).

**Updates:** We introduce another innovation in HMT: eventual consistency (EC). *dm-x* handles writes by updating the tree and then writing the data to the disk. While this works for smaller trees, such an approach reaches scalability limits as writes have a constant time complexity, and tree updates have a logarithmic one (with respect to tree size). EC in HMT relies on the idea that while tree updates provide enough throughput, they require latency hiding. Thus, instead of placing them on the critical path, we create a set of hashers that update the tree independently of the write requests. Specifically, for each write request, we store a per-sector tuple of [status, location, old IV, new IV], enabling us to complete write requests even if the tree update is not yet done. This makes the tree eventually consistent with the disk rather than continuously tracking its state.

While it resolves the latency issue, EC also needs to ensure a coherent state between disk and tree. In the case of parallel writes to the same location, the final state on the disk is nondeterministic as writes and their completions are asynchronous. Thus, we allow only one writer in each sector, synchronizing the writes and ensuring that the disk order agrees with the tree update order.

**IV cache design:** The hashers require all IVs within the same data set to conduct an update. To avoid reading hundreds of sectors and their IVs stored in the metadata of each sector, we introduced the metadata cache at the beginning of each SSD. We additionally use an in-memory, write-back cache based on these sectors. When a write happens to a given data set, we fetch the corresponding metadata sector into the IV cache and update it, keeping it always up-to-date with the state of the disk. It is crucial for performance as it allows reuse for sequential workloads. However, it also needs to maintain coherence with the disk and the tree. Both of these caches could be eliminated if the NVMe specification allowed reading just the metadata part of the sector instead of the whole sector.

**Crash recovery:** Ensuring crash recovery is an essential aspect of MTs. We provide free crash recovery for integrity, due to the NVMe standard, which guarantees the atomicity of writes per sector, including metadata. Such protection is not easily guaranteed for freshness, as the state of the MT is not atomically updated with the write to the disk. The strategy provided by *dm-integrity* or *dm-x* is to use journaling, which involves first reading and saving the old data to write the new one afterward. However, this approach introduces overhead for IOPS and throughput. We provide crash recovery leveraging our EC mechanism instead of journaling, gaining in algorithmic performance. Using the stored new and old IVs, we can ensure that the state of the tree can be recovered in case of a crash. However, all the

EC write requests need to be stored in persistently crash-protected memory, alongside the root of the tree. This can be achieved by introducing additional non-volatile SRAM to the remote sNVMe-oF. Such architectural change involves using a standard IP module [5, 13]. As each write takes up to 40us, even for 400Gbps, yielding 12.2 million packets per second, each requiring 24B, such a buffer requires only 7KB using the bandwidth-delay product. 7KB costs 3.5 cents, assuming the upper bound for SRAM price at \$5000/GB [51].

**4.3.2 Read path.** The request is first defined in the TEE and forwarded to the remote JBOF, where it is read from the disk. Once completed, freshness checks are conducted.

**Verification:** sNVMe-oF introduces a novel idea of a freshness fast path. During writes, alongside the data, we also store in the sector’s metadata a secure authentication hash binding the IV and the parent’s hash from HMT. The verification of HMT first compares the parent of the given node with the authenticated hash in the metadata. If these fit, the freshness checks conclude. If these are missed, a complete freshness check needs to be conducted. A complete freshness check involves fetching the metadata block into the in-memory IV cache and checking the IVs with the IV read from the disk. Freshness misses occur if a prior write has updated the parent hash and made the metadata freshness cache stale. To avoid it, one can conduct only large writes or periodically run a job to ensure the metadata cache in each block is up to date (like thrashing in HDDs). After freshness checks, the request is prepared for network freshness, like for writes, but with the complementary counter. After arriving at the local sNIC, the data is decrypted, verified, and delivered to the TEE using local secure communication (e.g., TDSP).

## 5 sNVMe-oF’s implementation

We prototyped sNVMe-oF on top of SPDK [87]. SPDK allowed us to conveniently expose sNVMe-oF instances as virtual block devices (vbdevs) while ensuring maximum performance and avoiding the kernel. Our implementation has around 6K lines of code that we release. We used AES-GCM for encryption and BLAKE3 [19] for hashing.

**Local instance:** We implemented the local sNVMe-oF service on top of an NVIDIA Bluefield3 Data Processing Unit (DPU) [24]. To access DPU’s cryptographic Generic Global Accelerators (GGA), we leveraged NVIDIA Data-Center-on-a-Chip Architecture (DOCA) [65]. We resolved some of the limitations of DOCA and modified SPDK to cooperate efficiently with it. Write requests arrive in the local sNVMe-oF vbdev as iovec buffers with no metadata fields. This data needs to be provided to the GGA accelerators as DOCA tasks. However, any buffers provided to DOCA must first be registered with its `mmap` function. Putting this on the critical path is not viable as it takes an order of milliseconds to complete. Thus, we modified the SPDK buffer pool to register the SPDK malloced memory with DOCA a priori. We

then exposed this mapping globally so that our vbdev could access it a couple of layers higher in the stack. Our approach is mappable to future applications requiring a combination of SPDK and DOCA buffers. While sharing source and destination buffers is typically optimal, in DOCA, these two must be different, which requires the introduction of temporary buffers allocated from a pre-registered buffer pool. We found that temporarily copying incoming requests to separate source buffers can bring more than 20% performance overhead as the DPU cores are relatively weak.

Such data movement cost is also the main reason we avoided using associated data (AD), as it requires copying the data to a temporary buffer and placing AD before the source buffer to conform with the DOCA format. We avoided AD in a novel manner by splitting the underlying encryption algorithm IV between the sector number and the actual IV. For our AES-GCM, the IV is 96 bits long, where we allocate the top 38 bits for sector numbers (1.13PB of storage) and the bottom 58 bits for the IV ( $1.18 \cdot 10^6$  PB of write capacity).

DOCA cryptographic tasks only support contiguous buffers that result in a single hash. Thus, we define tasks per storage sector. We batch these tasks and their completions together to alleviate the pressure of doorbelling the GGAs. We also batched writes/reads by waiting to complete all the corresponding single-sector tasks and sending one write/read. We found such a setup to be more performant than splitting requests into single-sector requests.

**Remote instance:** We implement an asynchronous least recently used (LRU) IV cache using a combination of a hashing map and a double-linked list. This combination enables  $O(1)$  lookups (hash map) and LRU insertions (double-linked list) while not considerably increasing the memory requirements of the cache. To ensure thread safety, we lock the whole cache on seek operations, an efficient mechanism that does not cause bottlenecks as our seeks are  $O(1)$ .

If a cache entry is not present, it can be scheduled to be read. After completion, callbacks for each requester would be run on their corresponding SPDK threads. Each cache entry has a lock used for hashing or reading the underlying values. Reads or writes accessing a given block move it to the beginning of the LRU list. If a new cache entry is needed, the last entry in the LRU list is written back, the entry is pushed to the LRU beginning, and the data is replaced with the requested sector. The new cache block is hashed and verified with the in-memory HMT to ensure freshness.

We implement HMT as an array of hashes, each with a corresponding `atomic_bool` lock located in an additional array. During writing, we conduct the eventual consistency with three POSIX threads that work similarly to an asynchronous accelerator. Tasks are scheduled in a round-robin manner between the threads that traverse the tree until the root is reached. We implement implicit ordering using the index within the array of locks to avoid update deadlocks.

## 6 sNVMe-oF’s evaluation

We address the following research questions:

1. What sNVMe-oF’s overheads for synthetic patterns?
2. How does the performance of the freshness read path change as the metadata cache gets polluted?
3. What is the impact of eventual consistency on writes?
4. What is the influence of sNVMe-oF on applications?

### 6.1 Experimental setup

We leverage two hosts: one representative of a tenant and one of a storage machine. The former is a single socket, 16-core, double hyperthreaded AMD EPYC 7313P with 2x16GB 3200MT/s DDR4 memory running Ubuntu 22.04.5 LTS and Linux 5.15. The latter is a double socket, 40-core, double hyperthreaded Intel Xeon Platinum 8460Y+ with 8x16GB 4800MT/s DDR5 memory running Ubuntu 22.04.5 LTS and Linux 5.15. The tenant has a 1.6TB Samsung MZPL1T6HEHP configured in 4KiB sectors without any metadata, while the storage server has a 3.84TB Western Digital DC SN655 configured into 4KiB sectors with 64B of metadata. For the former, we used a 100 GB `lvm` partition to measure performance, while the latter has been used unformatted. Both are equipped with an NVIDIA BlueField-3 (BF3) NIC and are connected back-to-back with a 100Gbit Ethernet link. The tenant BF3 is configured as a DPU, while the storage BF3 is configured as a NIC. The DPU is a 16-core ARM Cortex-A78AE with 32GB 5200 MT/s DDR5 memory running Ubuntu 22.04.5 LTS and Linux 5.15. The tenant and its BF3 use MOFED 24.10 and DOCA 2.9, while the storage server and its BF3 use MOFED 24.07 and DOCA 2.8. We used GCC version 11.4, SPDK version 23.01 commit 34edd9f1b, BLAKE3 version 1.8.2 commit 3a90f0f. For each experiment, we used 10 seconds of data and used at least 10 iterations.

### 6.2 Synthetic read performance

We evaluated the performance of sNVMe-oF when running different read patterns using `fio`’s SPDK backend. These represent different types of workloads. Baremetal is a deployment without any security. Integrity is demonstrated by using only the local sNVMe-oF instance to guarantee integrity. Freshness leverages both local and remote sNVMe-oF instances, providing integrity and freshness guarantees.

Figure 5 shows throughput, IOPS, and latency for three systems. Starting with throughput, we observe how sNVMe-oF provides both integrity and freshness at a cost of just 1-2%, reaching the size of network noise. The lower initial throughput is caused by insufficient saturation of the protection pipeline. As our latency increases for each request, we require higher throughput to hide it (e.g., encryption units on the BF3). The overheads for throughput are lowest because for larger reads, the proportion of time spent on any checks is smaller than in other cases. IOPS for random and sequential patterns show a similar trend, where the

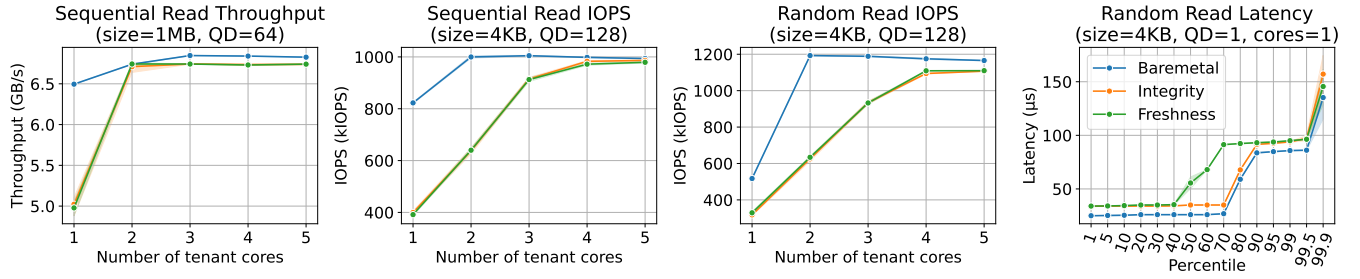


Figure 5. Performance of sNVMe-oF across different read patterns.

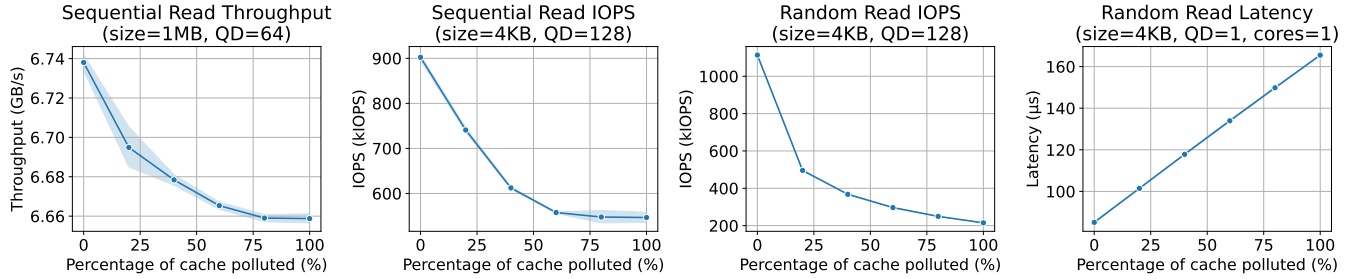


Figure 6. Scaling of freshness performance as we modify the proportion of the metadata cache that is polluted.

protection pipeline requires 4-5 cores to match bare metal performance. IOPS start with an overhead of 40-50%, which decreases to 1-2% for sequential reads and 5% for random reads. In both cases, freshness costs around 1% performance overhead. The jobs using a single core averaged 6% CPU usage with each additional core representing a 3 percent point increase regardless of whether sNVMe-oF has been used. These results are considerably better than existing methods, which for sequential reads can use up to 60% of the CPU (Figure 2) while losing 12% of the performance and providing fewer guarantees than sNVMe-oF. Similarly, for IOPS, at the same resource level, we achieve 5-6% overheads rather than 30%. For latency, we achieve similar performance.

Latency overheads for integrity stay within 30% of bare metal and reach around 10% overhead at the higher percentiles. The almost constant 9us overheads are caused mainly by the encryption. For freshness, these overheads grow earlier as additional checks are conducted on the data, such as comparing them to the tree values, and adding network freshness protections. These can create contention, which results in a shift in the distribution. Freshness behaves identically to integrity, apart from percentiles 50-80, where the overheads vary between 30 and 260%.

### 6.3 Impact of metadata cache pollution

In the previous experiment, we assumed an entirely fresh metadata cache for freshness. However, this is not always the case. Understanding how the overheads scale with the degree of dirtiness of this metadata cache is critical. Figure 6

shows how the performance of different patterns scales with the percentage of blocks that have a polluted cache with four tenant cores. Zero percent pollution implies a fresh cache, while 100% pollution implies a system without our metadata cache novelty. We observe that throughput is not considerably impacted by the pollution and drops only by 1%. This behavior is expected, as the requests require, on average, only one additional metadata sector read for many data reads. However, both IOPS and mean latency are considerably impacted. For sequential reads, the main issue is contention in the metadata cache, where multiple threads are serialized when locking the corresponding cache entry. For random reads, the issue is the ratio of metadata and data transferred. On average, each random write will require a write-back of the existing cache entry and a subsequent read of the metadata sector, followed by the actual read. This also considerably increases the latency with a polluted cache.

### 6.4 Synthetic writes and eventual consistency

Figure 7 shows the same 3 for write patterns. In these, we also differentiate two freshness sets: one with eventual consistency (w/ EC) and one without (w/o EC). Throughput shows a similar pattern to reads, with overheads of integrity and freshness reaching 2% and 3%, respectively. Integrity IOPS reach top performance at just two cores and achieve average overheads of 1% for sequential and random writes.

Freshness shows considerably worse overheads for IOPS, which reach 20-60% for the sequential pattern and 70% for the random one. Two reasons cause these larger overheads for

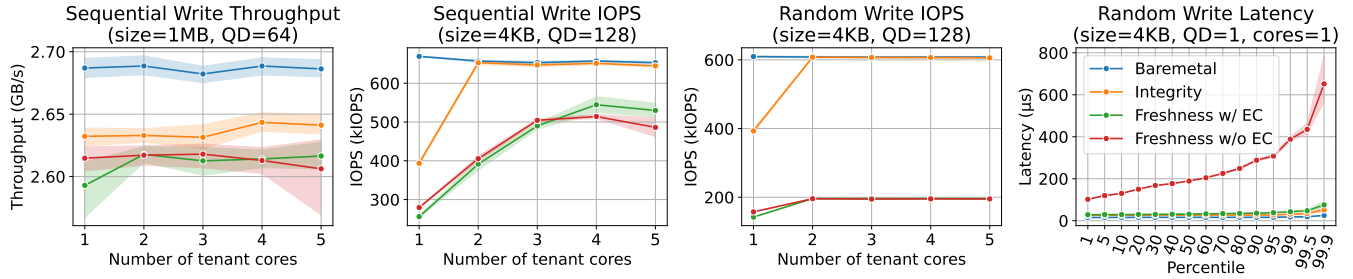


Figure 7. Performance of sNVMe-oF across different write patterns.

sequential writes. First, crash protection requires copying the old IVs as long as these are in memory. This implies contention as multiple threads lock the same cache entry in small sequential writes. Second, as the tree updates are conducted in an atomic fashion, contention is going to occur for small sequential writes happening on similar tree paths. The overhead for random writes IOPS is so large because for any tree update, we require all of the IVs of neighbors. For sequential patterns and large writes, this means we conduct a single read of the metadata IV sector to our in-memory cache, followed by many reuses of the sector or a large write. For a random pattern, there is little reuse. As we use half the bandwidth for metadata sectors, this more than halves IOPS. While we can hide additional latency in sequential writes, we cannot hide higher bandwidth usage in random writes.

Overall, the eventually consistent version performs as well as or better than the non-eventually consistent one. For IOPS, the performance difference reaches 6% of the bare metal performance. For latency, it is hundreds of percent. This is expected as placing the tree off the critical path hides the overheads. The overheads of the eventually consistent version above bare metal are larger than for reads, reaching 14us for low percentiles and 28-50us for the high ones. Integrity remains close to integrity, adding 10-11us for the low overhead case, and reaching 60% overheads.

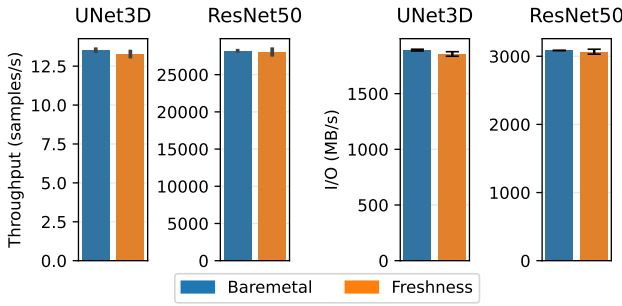


Figure 8. Overheads for an ML training pipeline.

## 6.5 Application performance

We deployed an ext4 file system on our disk and leveraged MLPerf’s storage benchmark [12, 21] to evaluate the impact of sNVMe-oF on the performance of machine learning (ML) training pipelines. These types of workloads have been deployed on disaggregated storage [88]. For our evaluation, we used ResNet50 and UNet3D, run over five epochs. For the former, we simulated training with 16 NVIDIA H100 GPUs over 2557 data files, each 137MB in size. For the latter, we simulated training with 1 NVIDIA H100 GPU over 3500 data files, each containing 140MB samples.

Figure 8 shows the performance of these models for the baremetal and freshness cases (with eventual consistency) across two metrics of interest: throughput of training samples, and the corresponding IOs. The former represents the end-to-end effective impact, while the latter a storage impact. The overhead of freshness remains at 1-2%. These workloads are predominantly large reads, which confirms the synthetic benchmark results in a practical deployment.

## 7 Related work

**CC storage:** Frameworks porting applications to TEEs typically provide storage solutions. Gramine [81], Occlum [77], and SCONE [18] offer protections by encrypting and hashing the files transparently. SecureFS [49], DIKSHIELD [15], and Intel’s IPFS [2] create secure file systems specific to SGX. We considered approaching the issue from the file system level, rather than the block device level. However, we found that synchronization of protections on the disaggregated file-system level creates a larger scalability problem compared to using the block device layer. Haven [22] provides protections on the block level in a similar fashion to *dm-integrity*. However, it does not handle freshness, is not TEE agnostic, and is fundamentally not designed for disaggregated storage.

**Integrity trees:** *dm-x* [25], Bonzai MTs [72], and ProMT [16] propose different MTs to protect local storage. Integrity trees are also used for securing non-volatile memory [36] and volatile memory in TEEs such as SGX [38]. VAULT [79] introduces a new type of tree organization that is more compact and minimizes depth. Counters can be used to achieve a similar performance improvement [74].

EnclaveDB [71] uses an integrity tree to ensure freshness for a database log. Most of these works are orthogonal to sNVMe-oF, focused on CC disaggregated storage optimizations.

**Distributed storage:** Works such as LustreFS [11], GPFS [75], HDFS [23], Ceph [84], and GFS [58] provide distributed storage scalable to thousands of storage nodes. Others like Octopus [54], Clover [82], Assise [17], and Orion [86] aim at optimizing the performance of different deployments. Some works also focus on storage smart NIC offloading. LineFS [46] introduces distributed file system offloading through sNIC pipelining. NVIDIA SNAP [14] virtualizes NVMe through hardware acceleration. Gimbal [61] optimizes the fairness of disaggregated storage. None of these works focuses on secure storage with freshness.

## 8 Conclusions

We presented sNVMe-oF, a secure disaggregated storage solution. We introduce a control path that disaggregates the freshness checks and scales to PB-scale disks, and modify the data path to introduce novel concepts such as metadata cache and eventual consistency. These enable sNVMe-oF to achieve overheads as little as 2% while providing confidentiality, integrity, and freshness. Combined with our portable SPDK implementation and BF3 support, we believe sNVMe-oF is a fundamental step for the future of scalable CC in datacenters.

## Acknowledgments:

We thank NVIDIA for providing computational resources and hosting MC’s internship where sNVMe-oF was developed. This research also obtained funding from the “UrbanTwin: An urban digital twin for climate action: Assessing policies and solutions for energy, water and infrastructure” project, funded by the ETH-Domain Joint Initiative program in the Strategic Area Energy, Climate and Sustainable Environment, a donation from Intel Corporation, and grant (agreement PSAP, No. 101002047) from the European Research Council (ERC) under the European Union’s Horizon 2020 program.

## References

- [1] 2016. Introducing Lightning: A Flexible NVMe JBOF.
- [2] 2016. Overview of Intel Protected File System Library Using Software Guard Extensions. [www.intel.com/content/www/us/en/developer/articles/technical/overview-of-intel-protected-file-system-library-using-software-guard-extensions.html](http://www.intel.com/content/www/us/en/developer/articles/technical/overview-of-intel-protected-file-system-library-using-software-guard-extensions.html).
- [3] 2019. GPUDirect Storage: A Direct Path Between Storage and GPU Memory. <https://developer.nvidia.com/blog/gpudirect-storage/>.
- [4] 2021. NVMe over Fabrics (oF) Specification (Historical Reference Only) - NVM Express.
- [5] 2023. A Comparison between Battery Backed NV SRAMs and NOVRAMs | Analog Devices. <https://www.analog.com/en/resources/design-notes/a-comparison-between-battery-backed-nvnbspsrams-and-novramps.html>.
- [6] 2023. NVIDIA BlueField-3 SNAP for NVMe and Virtio-blk v4.1.0. <https://docs.nvidia.com/networking/display/bluefield3snap410>.
- [7] 2023. Samsung Talks 1 Petabyte SSDs: Thousands of Layers, Packaging Innovations | Tom’s Hardware. <https://www.tomshardware.com/news/samsung-talks-1pb-ssds>.
- [8] 2024. Data Processing Units (DPU) | Empowering 5G Carrier, Enterprise and Cloud Data Services. <https://www.marvell.com/products/data-processing-units.html>.
- [9] 2025. Data Encryption Options | Cloud Storage. <https://cloud.google.com/storage/docs/encryption>.
- [10] 2025. Intel® Trust Domain Extension Linux Guest Kernel Security Specification – Intel® Trust Domain Extension. <https://intel.github.io/ccc-linux-guest-hardening-docs/security-spec.html>.
- [11] 2025. Lustre. <https://www.lustre.org/>.
- [12] 2025. MLPerf Storage. <https://mlcommons.org/benchmarks/storage/>.
- [13] 2025. nvSRAM (Non-Volatile SRAM) | Infineon Technologies. <https://www.infineon.com/products/memories/nvsram-non-volatile-sram>.
- [14] 2025. SNAP. <https://docs.nvidia.com/networking/software/snap/index.html>.
- [15] Jinwoo Ahn, Junghee Lee, Yungwoo Ko, Donghyun Min, Jiyun Park, Sungyong Park, and Youngjae Kim. 2020. DISKSHIELD: A Data Tamper-Resistant Storage for Intel SGX. In *Proceedings of the 15th ACM Asia Conference on Computer and Communications Security (ASIA CCS ’20)*. Association for Computing Machinery, New York, NY, USA, 799–812. <https://doi.org/10.1145/3320269.3384717>
- [16] Mazen Alwadi, Aziz Mohaisen, and Amro Awad. 2021. ProMT: Optimizing Integrity Tree Updates for Write-Intensive Pages in Secure NVMs. In *Proceedings of the 35th ACM International Conference on Supercomputing (ICS ’21)*. Association for Computing Machinery, New York, NY, USA, 479–490. <https://doi.org/10.1145/3447818.3460377>
- [17] Thomas E. Anderson, Marco Canini, Jongyul Kim, Dejan Kostić, Youngjin Kwon, Simon Peter, Waleed Reda, Henry N. Schuh, and Emmett Witchel. 2020. Assise: Performance and Availability via Client-local NVM in a Distributed File System. In *14th USENIX Symposium on Operating Systems Design and Implementation (OSDI 20)*. 1011–1027.
- [18] Sergei Arnautov, Bohdan Trach, Franz Gregor, Thomas Knauth, Andre Martin, Christian Priebe, Joshua Lind, Divya Muthukumaran, Dan O’Keeffe, Mark L. Stillwell, David Goltzsche, Dave Evers, Rüdiger Kapitza, Peter Pietzuch, and Christof Fetzer. 2016. {SCONE}: Secure Linux Containers with Intel {SGX}. In *12th USENIX Symposium on Operating Systems Design and Implementation (OSDI 16)*. 689–703.
- [19] Jean-Philippe Aumasson, Samuel Neves, Zooko Wilcox-O’Hearn, and Christian Winnerlein. 2013. BLAKE2: Simpler, Smaller, Fast as MD5. In *Applied Cryptography and Network Security*, Michael Jacobson, Michael Locasto, Payman Mohassel, and Reihaneh Safavi-Naini (Eds.). Springer, Berlin, Heidelberg, 119–135. [https://doi.org/10.1007/978-3-642-38980-1\\_8](https://doi.org/10.1007/978-3-642-38980-1_8)
- [20] AWS 2025. *Data Encryption | Introduction to AWS Security*. AWS. <https://docs.aws.amazon.com/whitepapers/latest/introduction-aws-security/data-encryption.html>.
- [21] Oana Balmu. 2022. Characterizing I/O in Machine Learning with MLPerf Storage. *SIGMOD Rec.* 51, 3 (Nov. 2022), 47–48. <https://doi.org/10.1145/3572751.3572765>
- [22] Andrew Baumann, Marcus Peinado, and Galen Hunt. 2015. Shielding Applications from an Untrusted Cloud with Haven. *ACM Trans. Comput. Syst.* 33, 3 (Aug. 2015), 8:1–8:26. <https://doi.org/10.1145/2799647>
- [23] Dhruba Borthakur et al. 2008. HDFS Architecture Guide. *Hadoop apache project* 53, 1-13 (2008), 2.
- [24] Idan Burstein. 2021. Nvidia Data Center Processing Unit (DPU) Architecture. In *2021 IEEE Hot Chips 33 Symposium (HCS)*. 1–20. <https://doi.org/10.1109/HCS52781.2021.9567066>
- [25] Anrin Chakraborti, Bhushan Jain, Jan Kasiak, Tao Zhang, Donald Porter, and Radu Sion. 2017. Dm-x: Protecting Volume-level Integrity for Cloud Volumes and Local Block Devices. In *Proceedings of the*

8th Asia-Pacific Workshop on Systems (APSys '17). Association for Computing Machinery, New York, NY, USA, 1–7. <https://doi.org/10.1145/3124680.3124732>

[26] Guoxing Chen and Yinqian Zhang. 2022. MAGE: Mutual Attestation for a Group of Enclaves without Trusted Third Parties. In *31st USENIX Security Symposium (USENIX Security 22)*. 4095–4110.

[27] Pau-Chen Cheng, Wojciech Ozga, Enriquillo Valdez, Salman Ahmed, Zhongshu Gu, Hani Jamjoom, Hubertus Franke, and James Bottomley. 2024. Intel TDX Demystified: A Top-Down Approach. *ACM Comput. Surv.* 56, 9 (April 2024), 238:1–238:33. <https://doi.org/10.1145/3652597>

[28] Marcin Copik, Grzegorz Kwasniewski, Maciej Besta, Michal Podstawska, and Torsten Hoefer. 2021. SeBS: A Serverless Benchmark Suite for Function-as-a-Service Computing. In *Proceedings of the 22nd International Middleware Conference (Middleware '21)*. Association for Computing Machinery, New York, NY, USA, 64–78. <https://doi.org/10.1145/3464298.3476133>

[29] Victor Costan and Srinivas Devadas. 2016. Intel SGX Explained.

[30] Jesse De Meulemeester, Luca Wilke, David Oswald, Thomas Eisenbarth, Ingrid Verbauwhede, and Jo Van Bulck. 2025. BadRAM: Practical Memory Aliasing Attacks on Trusted Execution Environments. In *46th IEEE Symposium on Security and Privacy (S&P)*.

[31] Yucong Duan, Guohua Fu, Nianjun Zhou, Xiaobing Sun, Nanjangud C. Narendra, and Bo Hu. 2015. Everything as a Service (XaaS) on the Cloud: Origins, Current and Future Trends. In *2015 IEEE 8th International Conference on Cloud Computing*. 621–628. <https://doi.org/10.1109/CLOUD.2015.88>

[32] Morris Dworkin. 2007. *Recommendation for Block Cipher Modes of Operation: Galois/Counter Mode (GCM) and GMAC*. Technical Report NIST Special Publication (SP) 800-38D. National Institute of Standards and Technology. <https://doi.org/10.6028/NIST.SP.800-38D>

[33] Morris Dworkin. 2010. *Recommendation for Block Cipher Modes of Operation: The XTS-AES Mode for Confidentiality on Storage Devices*. Technical Report NIST Special Publication (SP) 800-38E. National Institute of Standards and Technology. <https://doi.org/10.6028/NIST.SP.800-38E>

[34] Shufan Fei, Zheng Yan, Wenxiu Ding, and Haomeng Xie. 2021. Security Vulnerabilities of SGX and Countermeasures: A Survey. *ACM Comput. Surv.* 54, 6 (July 2021), 126:1–126:36. <https://doi.org/10.1145/3456631>

[35] Niels Ferguson and Bruce Schneier. 1999. A Cryptographic Evaluation of IPsec. (1999).

[36] Alexander Freij, Shougang Yuan, Huiyang Zhou, and Yan Solihin. 2020. Persist Level Parallelism: Streamlining Integrity Tree Updates for Secure Persistent Memory. In *2020 53rd Annual IEEE/ACM International Symposium on Microarchitecture (MICRO)*. 14–27. <https://doi.org/10.1109/MICRO50266.2020.00015>

[37] Avi Goldfarb and Catherine Tucker. 2012. Shifts in Privacy Concerns. *American Economic Review* 102, 3 (May 2012), 349–353. <https://doi.org/10.1257/aer.102.3.349>

[38] Shay Gueron. 2016. A Memory Encryption Engine Suitable for General Purpose Processors. *Cryptography ePrint Archive*, Paper 2016/204.

[39] Zerui Guo, Hua Zhang, Chenxingyu Zhao, Yuebin Bai, Michael Swift, and Ming Liu. 2023. LEED: A Low-Power, Fast Persistent Key-Value Store on SmartNIC JBOFs. In *Proceedings of the ACM SIGCOMM 2023 Conference (ACM SIGCOMM '23)*. Association for Computing Machinery, New York, NY, USA, 1012–1027. <https://doi.org/10.1145/3603269.3604880>

[40] Torsten Hoefer, Karen Schramm, Eric Spada, Keith Underwood, Cedell Alexander, Bob Alverson, Paul Bottorff, Adrian Caulfield, Mark Handley, Cathy Huang, Costin Raiciu, Abdul Kabbani, Eugene Opsasnick, Rong Pan, Adee Ran, and Rip Sohan. 2025. Ultra Ethernet's Design Principles and Architectural Innovations. <https://doi.org/10.48550/arXiv.2508.08906> [cs]

[41] Rambus Inc. [n. d.]. Rambus Delivers CXL 2.0 Controller with Industry-leading Zero-Latency IDE. <https://www.prnewswire.com/news-releases/rambus-delivers-cxl-2-0-controller-with-industry-leading-zero-latency-ide-301393137.html>

[42] Anuj Kalia, Michael Kaminsky, and David G. Andersen. 2016. Design Guidelines for High Performance {RDMA} Systems. In *2016 USENIX Annual Technical Conference (USENIX ATC 16)*. 437–450.

[43] Panos Kampanakis, Matt Campagna, Eric Crockett, Adam Petcher, and Shay Gueron. 2024. Practical Challenges with AES-GCM and the Need for a New Cipher. (2024).

[44] Mikhail Khalilov, Marcin Chrapek, Siyuan Shen, Alessandro Vezzu, Thomas Benz, Salvatore Di Girolamo, Timo Schneider, Daniele De Sensi, Luca Benini, and Torsten Hoefer. 2024. {OSMOSIS}: Enabling {Multi-Tenancy} in Datacenter {SmartNICs}. In *2024 USENIX Annual Technical Conference (USENIX ATC 24)*. 247–263.

[45] Jongyul Kim, Insu Jang, Waleed Reda, Jaeseong Im, Marco Canini, Dejan Kostić, Youngjin Kwon, Simon Peter, and Emmett Witchel. 2021. LineFS: Efficient SmartNIC Offload of a Distributed File System with Pipeline Parallelism. In *Proceedings of the ACM SIGOPS 28th Symposium on Operating Systems Principles (SOSP '21)*. Association for Computing Machinery, New York, NY, USA, 756–771. <https://doi.org/10.1145/3477132.3483565>

[46] Jongyul Kim, Insu Jang, Waleed Reda, Jaeseong Im, Marco Canini, Dejan Kostić, Youngjin Kwon, Simon Peter, and Emmett Witchel. 2021. LineFS: Efficient SmartNIC Offload of a Distributed File System with Pipeline Parallelism. In *Proceedings of the ACM SIGOPS 28th Symposium on Operating Systems Principles (SOSP '21)*. Association for Computing Machinery, New York, NY, USA, 756–771. <https://doi.org/10.1145/3477132.3483565>

[47] Ana Klimovic, Christos Kozyrakis, Eno Thereska, Binu John, and Sanjeev Kumar. 2016. Flash Storage Disaggregation. In *Proceedings of the Eleventh European Conference on Computer Systems (EuroSys '16)*. Association for Computing Machinery, New York, NY, USA, 1–15. <https://doi.org/10.1145/2901318.2901337>

[48] Hugo Krawczyk, Mihir Bellare, and Ran Canetti. 1997. *HMAC: Keyed-Hashing for Message Authentication*. Request for Comments RFC 2104. Internet Engineering Task Force. <https://doi.org/10.17487/RFC2104>

[49] Sandeep Kumar and Smruti R. Sarangi. 2021. SecureFS: A Secure File System for Intel SGX. In *Proceedings of the 24th International Symposium on Research in Attacks, Intrusions and Defenses (RAID '21)*. Association for Computing Machinery, New York, NY, USA, 91–102. <https://doi.org/10.1145/3471621.3471840>

[50] Reshma Lal, James B Anderson, and Andrew Jackson. 2023. Data Processing Unit's Entry into Confidential Computing. In *Proceedings of the 12th International Workshop on Hardware and Architectural Support for Security and Privacy (HASP '23)*. Association for Computing Machinery, New York, NY, USA, 56–63. <https://doi.org/10.1145/3623652.3623670>

[51] Mario Lanza, Sebastian Pazos, Fernando Aguirre, Abu Sebastian, Manuel Le Gallo, Syed M. Alam, Sumio Ikegawa, J. Joshua Yang, Elisa Vianello, Meng-Fan Chang, Gabriel Molas, Ishai Naveh, Daniele Ielmini, Ming Liu, and Juan B. Roldan. 2025. The Growing Memristor Industry. *Nature* 640, 8059 (April 2025), 613–622. <https://doi.org/10.1038/s41586-025-08733-5>

[52] Mengyuan Li, Yinqian Zhang, Huibo Wang, Kang Li, and Yueqiang Cheng. 2021. CIPHERLEAKS: Breaking Constant-Time Cryptography on AMD SEV via the Ciphertext Side Channel. In *30th USENIX Security Symposium (USENIX Security 21)*. USENIX Association, 717–732.

[53] Xupeng Li, Xuheng Li, Christoffer Dall, Ronghui Gu, Jason Nieh, Yousuf Sait, and Gareth Stockwell. 2022. Design and Verification of the Arm Confidential Compute Architecture. In *16th USENIX Symposium on Operating Systems Design and Implementation (OSDI 22)*. 465–484.

[54] Youyou Lu, Jiwu Shu, Youmin Chen, and Tao Li. 2017. Octopus: An RDMA-enabled Distributed Persistent Memory File System. In *2017*

*USENIX Annual Technical Conference (USENIX ATC 17).* 773–785.

[55] Jakob Luttgau, Michael Kuhn, Kira Duwe, Yevhen Alforov, Eugen Betke, Julian Kunkel, and Thomas Ludwig. 2018. Survey of Storage Systems for High-Performance Computing. *Supercomput. Front. Innov. Int. J.* 5, 1 (March 2018), 31–58. <https://doi.org/10.14529/jsfi180103>

[56] Ming Mao and Marty Humphrey. 2012. A Performance Study on the VM Startup Time in the Cloud. In *2012 IEEE Fifth International Conference on Cloud Computing*. 423–430. <https://doi.org/10.1109/CLOUD.2012.103>

[57] Garrett McGrath and Paul R. Brenner. 2017. Serverless Computing: Design, Implementation, and Performance. In *2017 IEEE 37th International Conference on Distributed Computing Systems Workshops (ICDCSW)*. 405–410. <https://doi.org/10.1109/ICDCSW.2017.36>

[58] Marshall Kirk McKusick and Sean Quinlan. 2009. GFS: Evolution on Fast-Forward: A Discussion between Kirk McKusick and Sean Quinlan about the Origin and Evolution of the Google File System. *Queue* 7, 7 (2009), 10–20.

[59] Jāmes Ménétrey, Christian Göttel, Anum Khurshid, Marcelo Pasin, Pascal Felber, Valerio Schiavoni, and Shahid Raza. 2022. Attestation Mechanisms for Trusted Execution Environments Demystified. In *Distributed Applications and Interoperable Systems: 22nd IFIP WG 6.1 International Conference, DAIS 2022, Held as Part of the 17th International Federated Conference on Distributed Computing Techniques, DisCoTec 2022, Lucca, Italy, June 13–17, 2022, Proceedings*. Springer-Verlag, Berlin, Heidelberg, 95–113. [https://doi.org/10.1007/978-3-031-16092-9\\_7](https://doi.org/10.1007/978-3-031-16092-9_7)

[60] Jesse De Meulemeester, Luca Wilke, David Oswald, Thomas Eisenbarth, Ingrid Verbauwhede, and Jo Van Bulck. 2024. BadRAM: Practical Memory Aliasing Attacks on Trusted Execution Environments. In *2025 IEEE Symposium on Security and Privacy (SP)*. IEEE Computer Society, 103–103. <https://doi.org/10.1109/SP61157.2025.00104>

[61] Jaehong Min, Ming Liu, Tapan Chugh, Chenxingyu Zhao, Andrew Wei, In Hwan Doh, and Arvind Krishnamurthy. 2021. Gimbal: Enabling Multi-Tenant Storage Disaggregation on SmartNIC JBOFs. In *Proceedings of the 2021 ACM SIGCOMM 2021 Conference (SIGCOMM '21)*. Association for Computing Machinery, New York, NY, USA, 106–122. <https://doi.org/10.1145/3452296.3472940>

[62] Masanori Misono, Dimitrios Stavrakakis, Nuno Santos, and Pramod Bhatotia. 2024. Confidential VMs Explained: An Empirical Analysis of AMD SEV-SNP and Intel TDX. *Proc. ACM Meas. Anal. Comput. Syst.* 8, 3 (Dec. 2024), 36:1–36:42. <https://doi.org/10.1145/3700418>

[63] msmbaldwin. [n. d.]. Overview of Managed Disk Encryption Options - Azure Virtual Machines. <https://learn.microsoft.com/en-us/azure/virtual-machines/disk-encryption-overview>.

[64] Dominic P. Mulligan, Gustavo Petri, Nick Spinale, Gareth Stockwell, and Hugo J. M. Vincent. 2021. Confidential Computing—a Brave New World. In *2021 International Symposium on Secure and Private Execution Environment Design (SEED)*. 132–138. <https://doi.org/10.1109/SEED51797.2021.00025>

[65] NVIDIA Corporation. 2025. *DOCA Documentation v2.10.0*.

[66] National Institute of Standards, Technology (NIST), Morris J. Dworkin, Elaine Barker, James Nechvatal, James Foti, Lawrence E. Bassham, E. Roback, and James Dray Jr. 00:11:00 2001. Advanced Encryption Standard (AES). <https://doi.org/10.6028/NIST.FIPS.197>

[67] PCI-SIG. 2022. TEE Device Interface Security Protocol (TDISP).

[68] Wei Peng, Yinshuai Li, and Yinqian Zhang. 2025. Shadows in Cipher Spaces: Exploiting Tweak Repetition in Hardware Memory Encryption. In *34th USENIX Security Symposium (USENIX Security 25)*. USENIX Association.

[69] Maria Petrescu and Anjala S. Krishen. 2018. Analyzing the Analytics: Data Privacy Concerns. *Journal of Marketing Analytics* 6, 2 (June 2018), 41–43. <https://doi.org/10.1057/s41270-018-0034-x>

[70] Sandro Pinto and Nuno Santos. 2019. Demystifying Arm TrustZone: A Comprehensive Survey. *ACM Comput. Surv.* 51, 6 (Jan. 2019), 130:1–130:36. <https://doi.org/10.1145/3291047>

[71] Christian Priebe, Kapil Vaswani, and Manuel Costa. 2018. EnclaveDB: A Secure Database Using SGX. In *2018 IEEE Symposium on Security and Privacy (SP)*. 264–278. <https://doi.org/10.1109/SP.2018.00025>

[72] Brian Rogers, Siddhartha Chhabra, Milos Prvulovic, and Yan Solihin. 2007. Using Address Independent Seed Encryption and Bonsai Merkle Trees to Make Secure Processors OS- and Performance-Friendly. In *Proceedings of the 40th Annual IEEE/ACM International Symposium on Microarchitecture (MICRO 40)*. IEEE Computer Society, USA, 183–196. <https://doi.org/10.1109/MICRO.2007.44>

[73] Mark Russinovich. 2023. Confidential Computing: Elevating Cloud Security and Privacy: Working toward a More Secure and Innovative Future. *Queue* 21, 4 (Sept. 2023), Pages 10:44–Pages 10:48. <https://doi.org/10.1145/3623461>

[74] Gururaj Saleshwar, Prashant J. Nair, Prakash Ramrakhyani, Wendy Elsasser, Jose A. Joao, and Moinuddin K. Qureshi. 2018. Morphable Counters: Enabling Compact Integrity Trees For Low-Overhead Secure Memories. In *2018 51st Annual IEEE/ACM International Symposium on Microarchitecture (MICRO)*. 416–427. <https://doi.org/10.1109/MICRO.2018.00041>

[75] Frank Schmuck and Roger Haskin. 2002. {GPFS}: A {Shared-Disk} File System for Large Computing Clusters. In *Conference on File and Storage Technologies (FAST 02)*.

[76] AMD Sev-Snp. 2020. Strengthening VM Isolation with Integrity Protection and More. *White Paper, January* 53 (2020), 1450–1465.

[77] Youren Shen, Hongliang Tian, Yu Chen, Kang Chen, Runji Wang, Yi Xu, Yubin Xia, and Shoumeng Yan. 2020. Occlum: Secure and Efficient Multitasking Inside a Single Enclave of Intel SGX. In *Proceedings of the Twenty-Fifth International Conference on Architectural Support for Programming Languages and Operating Systems (ASPLOS '20)*. Association for Computing Machinery, New York, NY, USA, 955–970. <https://doi.org/10.1145/3373376.3378469>

[78] Akshitha Sriraman and Abhishek Dhanotia. 2020. Accelerometer: Understanding Acceleration Opportunities for Data Center Overheads at Hyperscale. In *Proceedings of the Twenty-Fifth International Conference on Architectural Support for Programming Languages and Operating Systems (ASPLOS '20)*. Association for Computing Machinery, New York, NY, USA, 733–750. <https://doi.org/10.1145/3373376.3378450>

[79] Meysam Taassori, Ali Shafee, and Rajeev Balasubramonian. 2018. VAULT: Reducing Paging Overheads in SGX with Efficient Integrity Verification Structures. In *Proceedings of the Twenty-Third International Conference on Architectural Support for Programming Languages and Operating Systems (ASPLOS '18)*. Association for Computing Machinery, New York, NY, USA, 665–678. <https://doi.org/10.1145/3173162.3177155>

[80] Konstantin Taranov, Benjamin Rothenberger, Daniele De Sensi, Adrian Perrig, and Torsten Hoefer. 2022. NeVerMore: Exploiting RDMA Mistakes in NVMe-of Storage Applications. <https://doi.org/10.48550/arXiv.2202.08080> [cs]

[81] Chia-Che Tsai, Donald E. Porter, and Mona Vij. 2017. {Graphene-SGX}: A Practical Library {OS} for Unmodified Applications on {SGX}. In *2017 USENIX Annual Technical Conference (USENIX ATC 17)*. 645–658.

[82] Shin-Yeh Tsai, Yizhou Shan, and Yiyang Zhang. 2020. Disaggregating Persistent Memory and Controlling Them Remotely: An Exploration of Passive Disaggregated Key-Value Stores. In *2020 USENIX Annual Technical Conference (USENIX ATC 20)*. 33–48.

[83] W. Gregory Voss. 2017. European Union Data Privacy Law Reform: General Data Protection Regulation, Privacy Shield, and the Right to Delisting.

[84] Sage Weil, Scott A Brandt, Ethan L Miller, Darrell DE Long, and Carlos Maltzahn. 2006. Ceph: A Scalable, High-Performance Distributed File System. In *Proceedings of the 7th Conference on Operating Systems Design and Implementation (OSDI'06)*. 307–320.

[85] Tong Xing, Hesam Tajbakhsh, Israat Haque, Michio Honda, and Antonio Barbalace. 2022. Towards Portable End-to-End Network

Performance Characterization of SmartNICs. In *Proceedings of the 13th ACM SIGOPS Asia-Pacific Workshop on Systems*. ACM, Virtual Event Singapore, 46–52. <https://doi.org/10.1145/3546591.3547528>

[86] Jian Yang, Joseph Izraelevitz, and Steven Swanson. 2019. Orion: A Distributed File System for Non-Volatile Main Memory and RDMA-Capable Networks. In *17th USENIX Conference on File and Storage Technologies (FAST 19)*. 221–234.

[87] Ziye Yang, James R. Harris, Benjamin Walker, Daniel Verkamp, Changpeng Liu, Cunyin Chang, Gang Cao, Jonathan Stern, Vishal Verma, and Luse E. Paul. 2017. SPDK: A Development Kit to Build High Performance Storage Applications. In *2017 IEEE International Conference on Cloud Computing Technology and Science (CloudCom)*. 154–161. <https://doi.org/10.1109/CloudCom.2017.14>

[88] Yue Zhu, Weikuan Yu, Bing Jiao, Kathryn Mohror, Adam Moody, and Fahim Chowdhury. 2019. Efficient User-Level Storage Disaggregation for Deep Learning. In *2019 IEEE International Conference on Cluster Computing (CLUSTER)*. 1–12. <https://doi.org/10.1109/CLUSTER.2019.8891023>

## Appendix A: Design and implementation

**Offloading:** The main reasons for offloading were performance and resource usage improvements. These have also been supported by the ability to use GPU Direct file access, unlike local solutions, which require the data to go through the kernel. However, deploying sNVMe-oF control path on the sNIC also has its advantages. A service running on the host could also have obtained the tenant storage key and attested the remote sNICs. Importantly, tenant TEE needs to attest the local sNIC either way, as we leverage it as a security accelerator to ease the performance pressure on the host. Creating two services (one for acceleration and one for control path) would additionally increase the TCB, unnecessarily complicating the system design. The sNIC is a natural choice for a control path location, as all the data passes through it to the network, resulting in the least complicated system, with the smallest TCB and a combination of control and acceleration in one. A fully userspace deployment, avoiding any additional services, has the issues mentioned in the main text. Caching secure channels, keys, or counters is impossible, as a newly booted TEE has not been running earlier. Establishing these on boot would limit the scalability and increase startup complexity.

**Alternative layout for legacy drives:** We design sNVMe-oF with the typical 4096B datacenter SSD in mind and require 64B of metadata for all performance-improving features. However, we also offer a format for legacy drives that might offer only 16B of metadata, as shown in Figure 4. Such a format supports only 4.5PB of writes per key, suitable for smaller setups. It also does not support the fast-read path but enables other performance improvements for integrity and freshness. For this format, we still expose the drives over the network as having 64B of metadata to fit network freshness information. We then modify these requests accordingly on the JBOF to ensure only 16B is written to the SSDs.

**Disaggregating freshness:** We found the remote JBOF to be the only place to implement freshness checks while ensuring scalability. Placing HMT on the remote side implies no synchronization issues if all of the SSDs local to sNVMe-oF instance are managed by it. Such a design avoids expensive additional network bandwidth usage, especially for read-modify-write operations of our cache, and maintaining redundant copies of the tree in the memory of tenant instances. It also eases memory and compute pressure on the local sNIC occupied with encryption and integrity checking.

**RAID:** As one of the overheads we observe is bandwidth limitations, RAIDing our SSDs will improve sNVMe-oF’s performance. With RAIDed drives, the sectors are distributed between SSDs. Instead of leveraging additional metadata SSDs, putting all metadata blocks at the beginning of the drives avoids contention for access on the same disk, distributing the reads and writes of sNVMe-oF caches. It also increases the reliability of the system, as a single drive is not a point of failure.

**Deployment:** We spawn one instance of sNVMe-oF per sNIC and JBOF. sNVMe-oF then handles multiple tenants using different threads. Using multiple threads instead of separate processes per tenant minimizes context-switching overheads. These have been reported to take up to 29us [44], a considerable latency added on the critical path.

**Relaxing security and other properties:** While we design sNVMe-oF for the CC standards, not all applications require such strict security. sNVMe-oF can be expanded to these scenarios by disabling CC-specific features. The security levels can also be lowered in favor of a simplified design. For example, leaving out freshness requires only disabling the remote instance. As we developed sNVMe-oF on top of SPDK, it is also flexible enough to be deployed with local drives and combined with other properties such as fairness [61], to which sNVMe-oF’s bdev can attach.

## Appendix B: Further security considerations

**T10-DIF:** T10 Data Integrity Field (T10-DIF) is a basic mechanism that enables data integrity on the drives by leveraging additional NVMe metadata. T10-DIF can be used to verify if a block is read or written to the correct location and if its checksum is correct. T10-DIF requires trust to be put into the SSD, as it is where the checks are conducted. Its mechanisms are also not secure, as a simple checksum and block addresses can be modified without the user noticing. In contrast, sNVMe-oF provides strong security guarantees and does not trust the remote SSDs, thereby extending T10-DIF guarantees.

**Keys per IO:** Another feature that NVMe proposes is keys per IO, where the tenant provides their encryption keys to the SSDs during setup and then adds a key tag to each IO. The key per IO again requires trust in the SSDs, which accesses all the keys in plaintext. sNVMe-oF does not

require this while also being expandable to a key tag model. However, unlike in key per IO, sNVMe-oF enables even more granular potential for key management, where a key tag can be provided per block rather than the whole IO request.

**TDISP:** We leverage TDISP to extend trust into the local DPU in our work. The benefits of such an extension are the ability to use the accelerators on the DPU and enable performance optimizations such as GPU Direct. We explored the possibility of reusing in our design the security provided by PCIe Integrity and Data Encryption (IDE), which forms the basis of TDISP. However, this brings nontrivial challenges that would require hardware modifications. IDE is defined per virtual function (VF), and we do not have any influence over how the encryption happens. IDE also generates integrity for headers, which we cannot easily reproduce. While we cannot reuse the IDE, its addition is inexpensive. Even though there is currently no released

TDISP-capable setup to evaluate performance, IDE has been designed to work at line rate with certain products claiming zero bandwidth and latency overheads [41].

**Longer IV encryption schemes:** Recent encryption algorithms such as AEGIS256 have been designed to address the limited random IV write space we presented in Table 1. sNVMe-oF can also be extended to these. AEGIS256 has an IV of 256 bits with 128-bit blocks, allowing for  $7.7 \cdot 10^19$  PB of writes using random IVs. While simplifying the control path, such a large IV has shortcomings. As it is 32B, it would require 128B metadata to fit other parts of the sNVMe-oF format instead of 64B metadata per block. Such metadata size is not frequently found in SSDs. It would also require four times more space for the in-memory tree. Additionally, AEGIS is not yet standardized and is not yet supported by accelerators like the BF3 one we used.